CEAS Space Journal
https://doi.org/10.1007/s12567-023-00526-8

ORIGINAL PAPER

Analysis of the thermal design of a COTS-based modular battery system for satellites by thermal vacuum testing

Marius Eilenberger[1] · Hariharan Gunasekar[1] · Daniel Gomez Toro[1] · Cornelie Bänsch[1]

Received: 7 March 2023 / Revised: 15 September 2023 / Accepted: 18 September 2023

Abstract
The qualification of components for satellite applications is a costly process due to the extreme conditions that must be endured in space. Therefore, space market access of battery technology innovations is often inhibited. However, modern battery technologies offer great advantages for satellite applications. In this work, a commercial off-the-shelf (COTS) based and modular lithium-ion battery system for satellites in Low Earth Orbit (LEO) is presented. A comparative analysis to evaluate system parameters and functionality of the proposed battery system and literature data is performed. A thermal vacuum test campaign is carried out to investigate the behaviour under LEO relevant conditions and to achieve qualification of the system performance according to the ECSS (European Cooperation for Space Standardization) standard. The tested system consists of two modules with 28 V nominal voltage and eight battery cells each. Experiments were conducted inside a vacuum chamber. The battery system was charged and discharged in temperatures from 0 °C to 45 °C in a high-vacuum for three weeks. The influence of the battery management electronics, the behaviour of the cells and the heating were analyzed. The cell temperatures stayed in the operating limit during 3.5 A and 10 A cycling. The battery system, however, exceeded the cell's upper operating limit with a 40 °C baseplate and 3.5 A charging. Despite the dense system architecture with electronics between the cells the battery system can safely deliver power in a broad temperature range. Further investigations regarding safety and failure modes are necessary, along with advancements on software and state estimation algorithms.

Keywords Battery management system · Thermal vacuum · Thermal qualification · Satellite power

Abbreviations

BMS	Battery management system
BOL	Begin of life
CAN	Controller area network
CC	Constant current
COTS	Commercial of the shelf
CV	Constant voltage
DLR	German aerospace centre
DOD	Depth of discharge
DUT	Device under test
ECSS	European cooperation for space standardization
EoCV	End of charge voltage
EOL	End of life
FDIR	Failure detection, isolation and recovery
FMEA	Failure modes and effects analysis
LEO	Low earth orbit
LEOP	Launch and early operations
Li-ion	Lithium-ion
MSBS	Modular smart battery system
OBC	Onboard computer
PCB	Printed circuit board
PEEK	Polyether ether ketone
RUL	Remaining useful life
SOC	State of charge
SOH	State of health
TRL	Technology readiness level
TVAC	Thermal-vacuum
UART	Universal asynchronous receiver–transmitter

1 Introduction

In satellites the electrical power system is a crucial subsystem. It supplies, converts, stores and distributes energy on the satellite. Battery systems are usually the primary electrical power source during the eclipse, which is the phase

✉ Marius Eilenberger
Marius.Eilenberger@dlr.de

[1] DLR (German Aerospace Center), Institute of Engineering Thermodynamics, Energy Systems Integration, Pfaffenwaldring 38-40, 70569 Stuttgart, Germany

Published online: 11 October 2023

without sunlight during the orbit around Earth. Furthermore, a satellite's battery is used in the Launch and Early Operations (LEOP) phase and as a buffer for high-power consumers. Nowadays, lithium-ion (Li-ion) battery cells are typically applied due to their high volumetric and gravimetric energy density (of up to 250 Wh/kg) compared to other battery chemistries [1, 2].

The Li-ion cell, however, has disadvantages. The materials are rare, difficult to mine and toxic [3, 4]. Their minimum voltage (2.5 V) and maximum voltage (4.2 V) must not be exceeded to guarantee safe operation. In addition, the cell shall be stored between −20 °C and 60 °C and operated between 0 °C and 40 °C for most variants. Violating these limits can lead to reduced lifetime, outgassing or even fire [5]. Lastly, the lifetime or cycle stability of a Li-ion cell depends on the operation. A satellite in Low Earth Orbit (LEO) will experience around 6000 charge–discharge cycles just in a year [6]. Generally, the Li-ion satellite batteries of the past decade have worked successfully in-orbit for multiple years. They do so by reducing depth-of-discharge (DOD), EoCV (End of Charge Voltage), state of charge (SOC), current and avoiding temperature extremes [7].

The Li-ion battery for spacecraft was initially demonstrated in the Proba-1 mission [8]. The satellite, that originally was designed for one year, has now operated successfully for over 20 years with a battery system not exhibiting any battery monitoring or management. In ref. [8] the performance of the Li-ion battery systems of the Proba-1 and Mars Express missions is analyzed with ABSL in-house performance prediction tools. In general, the authors point out that the understanding of the changing behavior of the battery system over varied missions is crucial for an optimal battery sizing and with that a maximization of weight savings.

Since the flight on Proba-1 the Li-ion battery cell was validated as power storage for spacecraft and improved in energy density [9]. More and more satellite power systems switched from nickel–cadmium to Li-ion technology as it can be seen in a study by ESA [10]. Today the majority of spacecraft uses Li-ion cells.

However, a battery management system is rarely applied to date in space applications. A most prominent reason is the increase of complexity by the implementation of additional components and functionality into the system. Therefore, a failure modes and effects analysis (FMEA) is crucial to validate the safety requirements ensuring that the additional complexity does not lead to a decrease of the system's reliability.

On the other hand, the implementation of a battery management in satellite applications is supported by several arguments. Firstly, the advancements in technology enable the use of smarter and more energy-efficient electronics. Satellite battery systems, especially those of CubeSats, are including monitoring and managing for subsystems [11]. The advantages in safety, information need to outweigh the disadvantages. There are several publications available dealing with commercial of-the-shelf (COTS)-based battery systems [12, 13]. Secondly, the trend towards energy-dense battery cells paired with the rise of power requirements in satellite applications can be observed. With the application of a battery management system (BMS) in such systems mitigation of space debris can be achieved by following the standards for satellite applications [14]. A disbalance of the battery cells can lead to failure or worse [5]. Lastly, the knowledge on the SOC and state of health (SOH) of the battery cells gives the satellite operator more insight for problem solving or operations planning [15]. Especially for satellites, which cannot receive maintenance, an additional improvement and knowledge of the remaining battery lifetime is beneficial [16].

An overview of available literature data of Li-ion-based battery systems for satellites is shown in Table 1. The data are taken from refs [17–20].

Among the 22 named battery systems there are small ones that are focused on the CubeSat market and larger ones that are used in small and medium satellites. The smaller systems generally follow the COTS approach whereas the medium and large systems follow a more robust and conservative selection of components.

A simple balancing approach is implemented in 8 of the cited battery systems, which are both small and large systems. In those systems the cells are balanced over a shunt resistor at one prefixed voltage. Adaptive EoCV is offered by two systems.

Four battery systems offer SOC calculation via coulomb counting. One offer SOH monitoring.

Most systems do not state a radiation tolerance level. For five of the systems the TID value is between 20 and 30 krad, which allows 5-year LEO missions. An outlier is a battery system that offers radiation tolerance of up to 3000 krad.

The approach of using non-space qualified COTS electronic components and battery cells leads to higher efforts for qualification and testing under relevant conditions. In contrast, high energy densities (> 120 Wh/kg at battery system level), more functionality and lower prices can be achieved. There are also battery systems successfully flying in satellites that do not use battery management and balancing. The drawback is that these systems need more focus on battery cell selection and battery cell testing. The cells must to have the same interior resistances or a behaviour that keeps them balanced. The early Li-ion powered satellites relied on a specific mechanism of decreasing self-discharge with increasing SOC in their selected cell [21].

In this work, a modular COTS-based battery system is presented to achieve a first proof-of-concept. Its behaviour under thermal loads and vacuum relevant conditions

Table 1 Overview of available literature data for specifications and characteristics of Li-ion [17–20]

Name/Manufacturer	Weight [kg]	Vol. [l]	Grav. energy density [Wh/kg]	Balancing	SOC / SOH	Radiation [krad]
Crystalspace Vasik	0.14	0.11	157	No	No	N/A
Sputnik SXC-BAT	0.36	0.28	111	No	No	N/A
Satrevolution	0.49	0.28	112	No	SOC	N/A
GomSpace BP8	0.49	0.38	178	Analog	No	N/A
GomSpace BPX	0.5	0.33	150	No	No	N/A
Pumpkin BM2	0.7	0.50	143	No	SOC: 20% steps	N/A
SAFT 4S1P	0.7	0.59	91	No	No	N/A
SVC 39501	1.0	0.91	22	No	SOC	N/A
Skylabs Nanoeps	1.9	1.67	82	Active	No	N/A
BST Bat-110	3	2.48	57	Analog	SOC/SOH	30
Redwire Nova	3.3	3.15	138	Analog	No	N/A
EaglePicher15,5Ah	4.0	1.58	113	No	No	N/A
Ibeos B25-550	4	2.97	138	No	No	30
SatSearch VLB	4.5	3.30	77	Analog	No	20
SAFT LEO	5	4.99	102	Analog	No	N/A
Ibeos 50VkWHR	7.5	5.93	133	No	No	30
Ibeos B28	8	5.70	138	No	No	30
EaglePicher SAR	28.2	27.95	118	No	No	N/A
SAFT Small GEO	28.8	29.70	98	Analog	No	N/A
EaglePicher SAR	28.2	27.95	118	No	No	N/A
EaglePicher SAR	63.5	47.52	105	No	No	3000
SAFT MEO/GEO	69.6	68.92	131	Analog	No	N/A

is investigated. The battery system consists of electronics, battery cells and structure. An autonomous BMS is applied. The structure serves to support the stabilization and thermal aspects of the system. The electronics are mounted on a printed circuit board (PCB) that is in contact with the battery cells and also serves the structural integrity of the system. A market study supports the systems beneficial energy density and functionality considerations [22]. Thermal vacuum tests are conducted to investigate the system's behaviour under space-relevant conditions and to validate the conceptual approach.

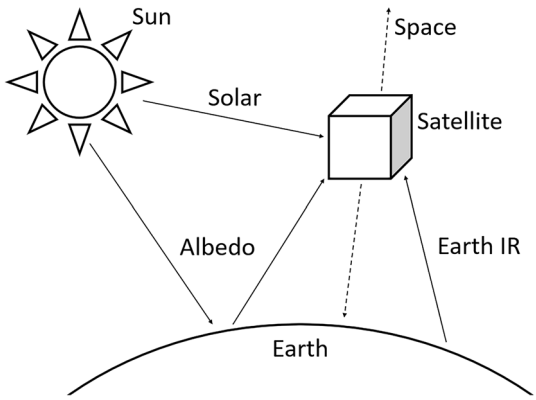

Fig. 1 In-orbit radiative influences on a satellite

2 Design of the battery system

2.1 Space environment

The environmental conditions and requirements to the battery system are a result of the mission and orbit of the satellite. The focus of this paper is on the vacuum condition and the temperatures that a battery system experiences in LEO.

The temperature of a spacecraft is influenced by four sources of energy [23]. The different radiation sources are visualized in Fig. 1. These are the Sun, Earth's albedo, Earth's infrared radiation and the internal electronic hardware. The Sun's solar flux goes directly to the hull of the satellite. The albedo is a fraction of solar energy which is reflected by Earth. Furthermore, Earth's surface absorbs radiation from the Sun. It then reemits a part of the energy as infrared. Lastly, the hardware onboard the satellite produces waste heat. The incoming energy then exchanges in form of heat between the satellite's shell and interior hardware like a battery system.

In a spacecraft heat is transferred via radiation and conduction. Convection does not happen due to the lack of air in high vacuum conditions.

During its orbit around the Earth a spacecraft experiences sunlight, during which the batteries are charged via solar cells, and a phase of no sunlight, called eclipse [24], in which the batteries are discharged. The temperature of a satellite in orbit varies depending on its position and therefore incoming radiation and also by the heat dissipated from the spacecraft's subsystems. In a thermal analysis the hot case and cold case investigate the most extreme temperatures that occur due to the external and internal heat sources.

Thermal systems in satellites mainly use passive elements. Colours of surfaces, conducting and isolating elements do most of the thermal control for subsystems. Often-used active thermal elements are heaters due to their low volume and simple implementation. Other active elements like heat pipes are only used for special missions or by large satellites [25].

2.2 Modular smart battery system (MSBS)

To achieve a modular and scalable architecture, the MSBS, proposed in this work, consists of separated battery modules connected in parallel by the surrounding structure. Each module contains battery cells, electronics and structural elements. The aspect of modularity is described in detail in a previous work [22]. In Fig. 2 the first prototype consisting of two parallel modules is shown. The PCBs with electronics are directly connected with the battery cells and include all necessary components to manage the cells. The aluminium thermal elements and structure elements are also visible. The PCBs also act as structural components and give stability to the system.

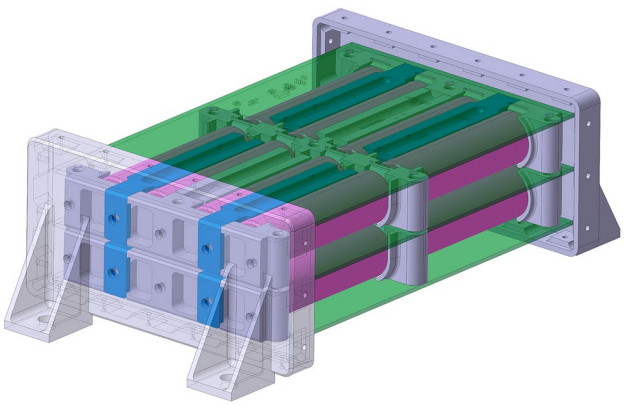

Fig. 2 Battery system with two battery modules and surrounding structure. Battery cells (pink), PCBs (green), thermal elements blue, structure elements (grey

The system delivers a nominal voltage of 28.8 V (with maximum of 33.6 V and minimum of 20 V), a maximum current of 10 A short term (< 1 min) and a continuous current of up to 3.4 A.

In Fig. 3 the volumetric and gravimetric energy densities of systems from literature are compared to the presented single module and the systems with structure and two or four modules. The MSBS with added battery management and compact structural elements exhibit high system energy. The battery modules use commercial components that are available in high quality at an affordable price (most components are below 10 €). The battery cells used are standard cells in the 18,650 size.

The battery system contains a BMS that balances the serially connected cells, monitors the charging and discharging currents and analyses the operating status of the cells. The values and status messages can be communicated via Controller Area Network (CAN) or Universal Asynchronous Receiver–Transmitter (UART) to the onboard computer (OBC), power control and distribution unit (PCDU) or even shared between the modules. Additionally, a command can be sent to the modules to change operation of balancer, heater or state machine.

The centrepiece of the BMS is a microcontroller that is programmed with the software and commands the other electronic components like temperature sensors, current sensor and heaters. A balancing unit individually measures and balances each cell voltage at any value. Moreover, there are components for communication via CAN, temperature measuring, current measuring, latch-up protection, voltage regulation, heating and a back-up balancer. These components have either been previously tested for radiation or have a rad-hardened counterpart. The software of the system, which runs the battery management, checks the sensors and runs a state machine. With this state machine the temperature, current and voltages of the battery cells are monitored, analyzed and managed. In case of an error or emergency possible actions are heating, balancing, reset of the system or ignoring a faulty sensor.

The battery system contains one temperature sensor on each battery cell. The temperature sensors are communicating with the microcontroller on a one-wire bus. The onboard software communicates the monitored temperature at a resolution of 1 °C. A higher resolution for the temperatures of up to 0.0625 K can be requested via CAN.

The structure components inside the battery modules are part of the thermal system (Fig. 2). There are cell holders that physically connect the battery cells with the PCBs and hold everything in place. The cell holders are 3D-printed with polyether ether ketone (PEEK). This material was selected for its low weight and good electrical isolation properties. The thermal surface between the battery cells and the outside structure is improved by the integration of

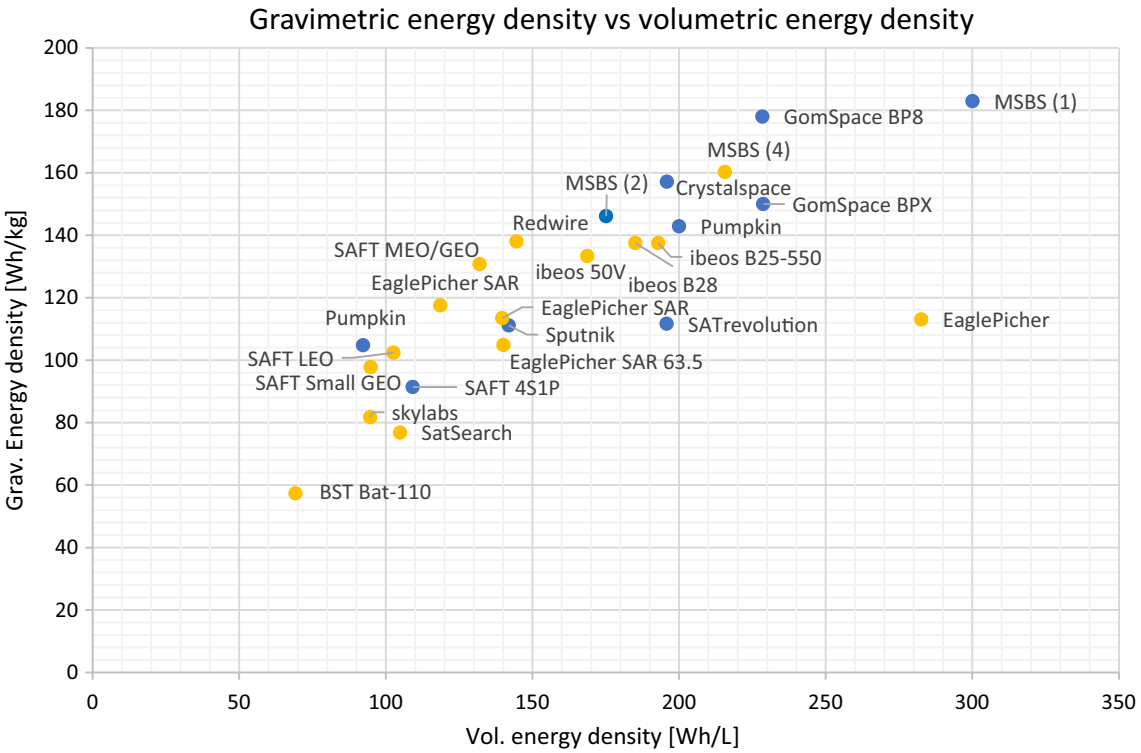

Fig. 3 Gravimetric versus volumetric energy densities of battery systems for satellites from literature compared to the systems of this work. MSBS (1): single battery module; MSBS (2): structure with two battery modules; MSBS (3): structure with four battery modules. Systems marked in blue are made for CubeSats (box-less integration) and systems marked in yellow are battery subsystems made for larger satellites. Literature data is taken from refs. [17–20]

thermal wedges, which are placed between the battery cells and are in direct contact with them and the structure. The thermal wedges are milled from aluminium, which is used for its good thermal conductivity. The aluminium wedges are not in contact with any of the battery cell's poles. A thermal paste is used to reduce the contact resistance of the connection between thermal wedges, battery cells and PCBs.

The cell holders, thermal wedges, and included heater elements can be seen next to the battery cells and PCBs in Fig. 4. The system is thermally and structurally connected to the satellite via the aluminium boards at each end of the system. They can also be seen in Fig. 4.

To prevent the module of too cold temperatures four heaters are implemented into the thermal structures on each module. The aim of this thermal design is to ensure that the battery cells can be operated in an acceptable temperature window in a satellite environment.

The functionality and modern components used in the system must not add fatal errors. The system was, therefore, designed redundant. A simple FMEA with failures of the most important components of the BMS is presented in Table 2. Generally, the battery cells can always be charged and discharged, even if the BMS is not powered or failed. In case of an onboard electronics failure the cells are still

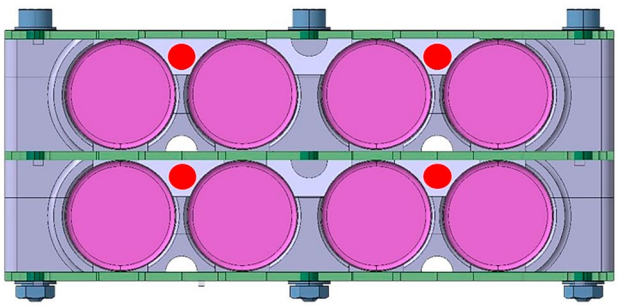

Fig. 4 Side view of the modular system with battery cells (pink), thermal wedges (light grey) and heater elements (red) next to the PCBs (green)

operable. A backup balancing based on analog shunts will work without the BMS. Two additional temperature sensors on each module can be read out by an external system like the Onboard Computer (OBC) or PCDU. Failure of a module can be compensated by additional modules and failure of a sensor can be compensated by the other sensors. As the battery system is powered externally and not by itself there is also an additional layer of safety. In case of malfunction the BMS can simply be deactivated.

Table 2 Top-level FMEA analysing the most critical failures in the battery system

Item/block	Failure mode	Failure cause	Failure effects	Failure detection method/observable symptoms	Compensating provisions	Severity number
Battery cell	Not connected	Open circuit	Loss of module	BMS does not detect cell or cell string, no power from module	1. Redundancy in modules	2
Battery cell	Loosing voltage	Short circuit	Loss of module	BMS detects rapidly decreasing voltage, increasing temperature	1. Safety mechanisms in the cell, circuit-break 2. Redundancy in modules	3
Balancing	Balancing unintendedly on	Software, Electronics	Voltages reducing, Temperatures Increasing	Balancing on, temperature sensors detect increase, voltage sensing detects decrease	1. Powercycling 2. Cut of power to BMS 3. Analog backup balancer	2
Balancing	Balancing not working	Software, electronics	Cells are not balanced	Voltages of cells stay apart, don't get balanced	1. Power cycling 2. Test of all functions 3. Analog backup balancer	2
Heating	Heating unintendedly on	Software, electronics	Temperatures increasing	Heater is constantly on, temperature increasing	1. Power cycling 2. Cut of power to BMS 3. Analog backup balancer	2
Temperature sensing	No or implausible value	Software, Sensor	System receives no or implausible value	Value is extreme and changed fast	1. Plausibility Check 2. Power cycling 3. Use other temp sensors	1

The entire electronics on the PCB is tested successfully until 35 krad.

The energy that is consumed by electronic components is dissipated as heat. Additionally, the battery cell's dissipated power or heat (P) can be calculated with their internal resistance (R) and operating current (I):

$$P = R \times I^2 \tag{1}$$

One cell has 0,06 Ohm of internal resistance according to the datasheet. At 3.5 A, eight cells dissipate around 6 W. Therefore, adding the average electrical consumption of each electronic component to the heat dissipated by the cells gives a good estimation of the overall heat dissipation. For one module this results in around 60 mW of dissipated heat. The electronics consumption happens due to a five second interval in which the BMS checks its sensors, calculates and communicates. Most of that five second interval the system is in sleep mode.

The stand-out characteristics of the developed battery system concept are the following:

- Modularity of the system in capacity, current and voltage
- Sensors, microcontroller and software for collection and processing of data
- Single cell voltage, current and temperature measurements for deep understanding and scientific research on cell behaviour in orbit
- Smart balancer with adaptable end of charge voltage (EoCV)
- Analysis of state of charge (SOC) and state of health (SOH) to infer on the remaining useful life (RUL)

3 Thermal vacuum campaign: experimental approach

3.1 Test setup

For the thermal-vacuum campaign several components were used to simulate the satellite's surroundings, energy flow and communication. The test setup is shown in Fig. 5.

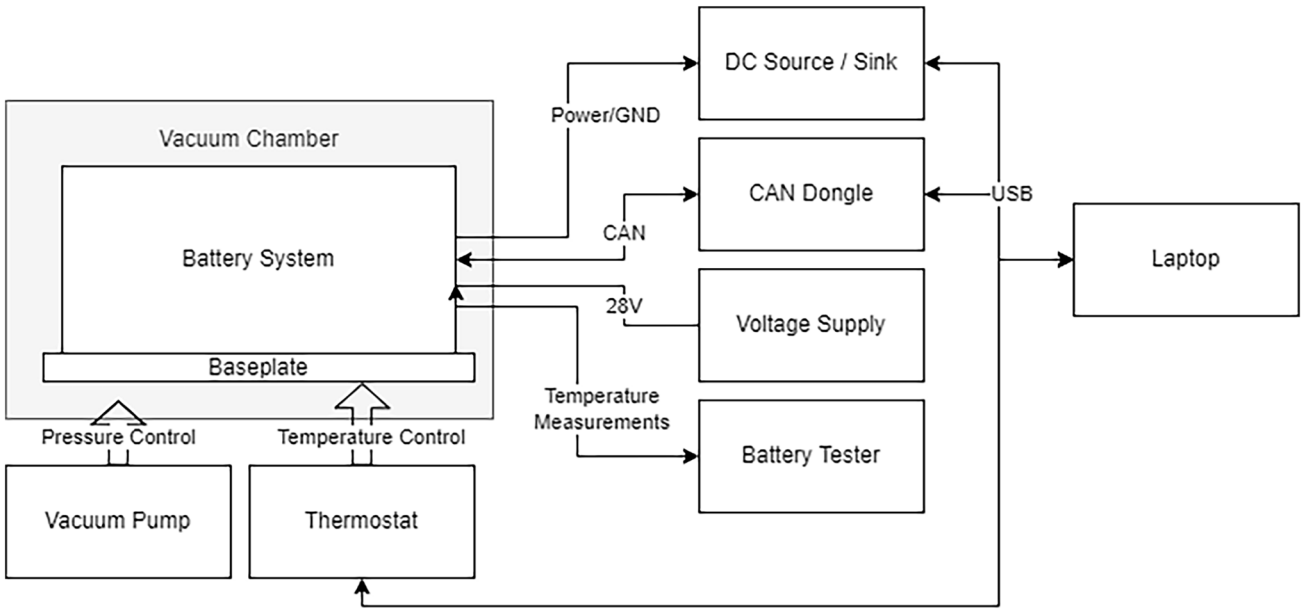

Fig. 5 Schematic diagram of the test setup for the thermal vacuum experiments consisting of vacuum chamber with thermostat and pump (left side), battery charging, discharging and monitoring (middle) and control laptop (right side)

The battery system was placed in the vacuum chamber and held constantly under vacuum for three weeks. The vacuum chamber is equipped with a vacuum pump and has a thermostat attached to it. The additional equipment consists of a remotely accessible laptop with LabVIEW as control and automation platform, an electrical source–sink combination (EA PSB 9080–120 with 0–120 V and 0.1% precision), a CAN dongle (PCAN-USB IPEH-002021 with 250 kbits/sec) and a battery tester (Basytec Cell Test System). With the laptop every test device of the setup can be controlled and the communication with the two battery modules in the vacuum chamber is routed to the laptop via CAN. The source–sink is used to charge and discharge the battery system. The 28 V supply simulates the power supply of the battery management's electronics. This enables an external reset of the BMS electronics. The battery cells are not connected to this and can still be charged or discharged if the voltage supply is turned off. Lastly, the battery tester was used to read out additional external temperature sensors. Eight external temperature sensors were placed on the battery system. Figure 6 shows their positions. Two of them are placed on the legs of the structure close to the baseplate (1,2). Two sensors are placed inside the thermal elements (3,4). Two additional external sensors are placed next to on-board sensors (5,6,7) to validate the temperature measurement on the battery cells. The last external sensor is placed inside the top module at the pole of a cell (8).

The collected data via CAN bus include current, voltages and temperatures of the system. Additionally, status messages that describe the system state (charging, discharging, idle, balancing and emergency) and the status of the balancer and heater are logged. Every five seconds a dataset is collected via CAN bus and stored on the laptop. In addition, voltage and current of the source and sink were measured. Therefore, each measured value of the onboard sensors can be compared to the external measurements. With this setup the temperatures and currents could be changed remotely and the system can be monitored at any time.

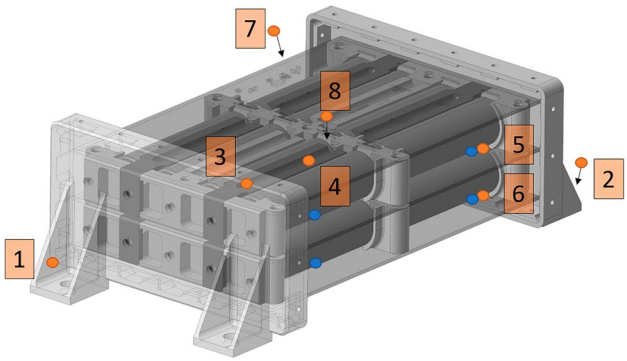

Fig. 6 Visualization of the external temperature sensors (orange). External temperature sensors 1–4 are placed next to the BMS's onboard (blue) temperature sensors that monitor the cells. Only four of the on-board cell sensors are shown in the graph

To emulate the environmental conditions, the battery system including battery cells was placed on a thermal baseplate. The test setup with baseplate (copper) and battery system can be seen in Fig. 7. The blue cables are connected

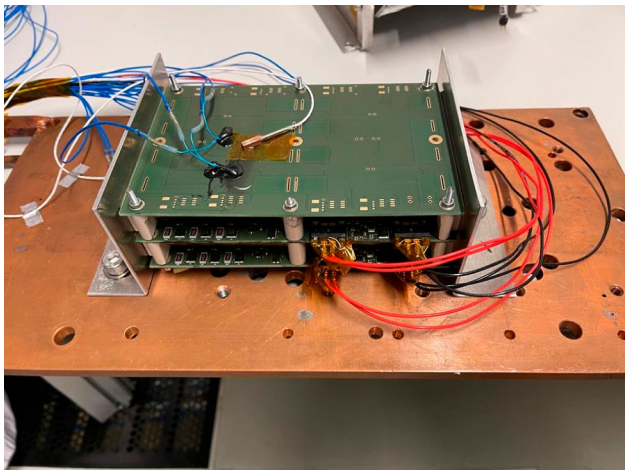

Fig. 7 Picture of the test setup of two battery modules and structure

to the temperature sensors. The red and black cables are used for charging and discharging of the system.

The temperature of the thermal baseplate can be controlled with a heat transfer fluid. This fluid is regulated from the outside by a thermostat. Before insertion into the vacuum chamber the setup was additionally surrounded by a thermal shroud. The thermal shroud reflects thermal radiation back to the battery system. The baseplate simulates the mechanical interface and thermal conduction with the satellite. The shroud simulates the thermal radiation inside of the satellite. The satellite interfaces and in-orbit temperatures could deviate from the test setup. However, the connection and thermal management of the satellite are usually designed to benefit the most sensitive components.

The temperatures of the baseplate were changed during the test according to the test plan. The temperature of the shroud was also monitored and was within 4 K of the baseplate after the dwelling and during the tests.

The goals for the thermal-vacuum test campaign are as follows:

- Prove operation of battery cells in thermal-vacuum.
- Prove functionality of electronics in thermal-vacuum.
- Test battery system under different static temperatures during charging and discharging.
- Understand thermal behaviour and heat distribution of the battery system during operation.

3.2 Testing process

The thermal-vacuum campaign was based on to the ECSS standard [26, 27]. At first a non-operational cycle was conducted. In this the baseplate and system were tempered to the non-operational limits (−20 °C and 60 °C). Then the temperatures were held (dwelling). In the non-operational cycle the battery cells were not charged or discharged, but the monitoring and BMS was turned on.

Thereafter seven operational cycles were conducted. For each of the seven operational cycles (thermal cycles) the operational maximum (40 °C) and the operational minimum (0 °C) were approached and held. After each temperature change, once the temperature had settled, charging and discharging of the battery system was conducted (electrical cycles). During the whole campaign a two-hour dwelling was conducted after each temperature change. The dwelling was only started if all temperatures were measured within 1 K or beyond the goal temperature. For the operational maximum 40 °C instead of 45 °C was chosen due to the heating from the cells during the electrical cycling.

Charging and discharging was conducted with the two battery modules connected in parallel. The system's battery cells were charged and discharged at a baseplate fixed temperature after the dwelling was completed. Two different currents were applied during the tests. One cycle consisted of discharging and charging of the battery system. The battery cells were charged to 32.8 V, which is the product of eight serial battery cells at 4.1 V (approx. 90% SOC). The charging process consisted of a constant current (CC) phase and a constant voltage (CV) phase until a charging current of 300 mA was undershot.

At least four cycles for each temperature–current combination were carried out to give the system time to approach a thermal equilibrium.

The temperature ranges for the battery system are limited by the temperature limits of the battery cells themselves. Li-ion cells generally have two temperature ranges. The non-operational temperature range for storing the cells, usually ranges from −20 °C to 60 °C [28]. The operational range is between 0 °C and 45 °C for charging and broader for discharging (−20 °C to 60 °C). The operational range is smaller because the cells are additionally stressed internally. These temperature limits must not be exceeded during the test or the operation due to safety reasons. There is an optimal range for operating between 10 °C and 35 °C. Anything that goes far from this causes an accelerated aging of the cells [29]. The eight thermal cycles including the temperature changes and dwell times took about ten days of continuous monitoring and testing. Additional tests included discharging at −20 °C and 55 °C and tests for the heating and balancing. The aspired pressure inside the vacuum chamber is at 10^{-6} mbar or lower.

The stability of the microcontroller and electronics were also tested and evaluated during the thermal vacuum test campaign. The on-board data logging, processing and communication and the functions of the electronics like heating and balancing were tested. The system temperatures are monitored (Table 3).

Table 3 Testing parameters

Parameter	Value
Pressure	$< 10^{-6}$ mbar
Temperature	0 °C to 40 °C
Current	3.5 A & 10 A
Additional Test	Discharging −20 °C Discharging 55 °C Heating & Balancing

4 Results

4.1 Influence of current on temperature

Figure 8 shows the results of the electrical cycling during the 40 °C operational test of a thermal cycle. The measurements of current and temperatures of the external sensors in relation to the testing time are visible. The test started at 40 °C baseplate temperature (therefore simulating a 40 °C connection interface to the satellite). The temperature control for the extreme temperatures is hard to achieve with losses between thermostat and baseplate. Therefore, a more extreme temperature was also accepted to start the dwelling or cycling. The measured current is the module current which flows through each cell. In the graph five cycles are depicted. One cycle consists of charging and discharging. The discharging leads to a temperature increase.

The temperatures also increase during CC phase. During the CV phase the temperatures decrease. The pronounced temperature increase during discharge and CC phase is the consequence of the heat dissipation that stems from the current flowing through the cells and their interior resistances. The temperatures decrease slightly during the CV phase as the current through the battery cells and therefore the heat dissipation is rapidly decreasing. During that phase the thermal conduction away from the battery cells is greater than the thermal heat dissipation generated inside of the battery cells due to the internal resistance.

The baseplate and, therefore, the emulated satellite are heated to 40 °C. This can be seen in the baseplate connection sensors, which stays between 41–42 °C for the whole test as it is very close to the baseplate. It also has to be noted that there are temperature differences between certain parts of the battery system. Firstly, a temperature difference of around 1 K can be seen between baseplate and the battery system's structure. Further, a temperature difference of around 1.5 K can be observed between the structure and the thermal elements. Finally, a gap in temperature of below 1 K between the thermal elements and the battery cells is visible.

Altogether, the temperature increases during the first two cycles. At the beginning of the experiment the overall temperature increase is pronounced. After cycle three, an equilibrium seems to be reached. This means that a thermal balance between inflowing energy in the form of dissipated heat from cells and electronic is almost equal to the outflowing energy via thermal conduction and thermal radiation. Conduction and radiation of heat to the outside increase with rising temperature. It is assumed that both processes contribute to the equilibration.

The maximum temperature difference between baseplate and battery cells amounted to 4.5 K in this particular test.

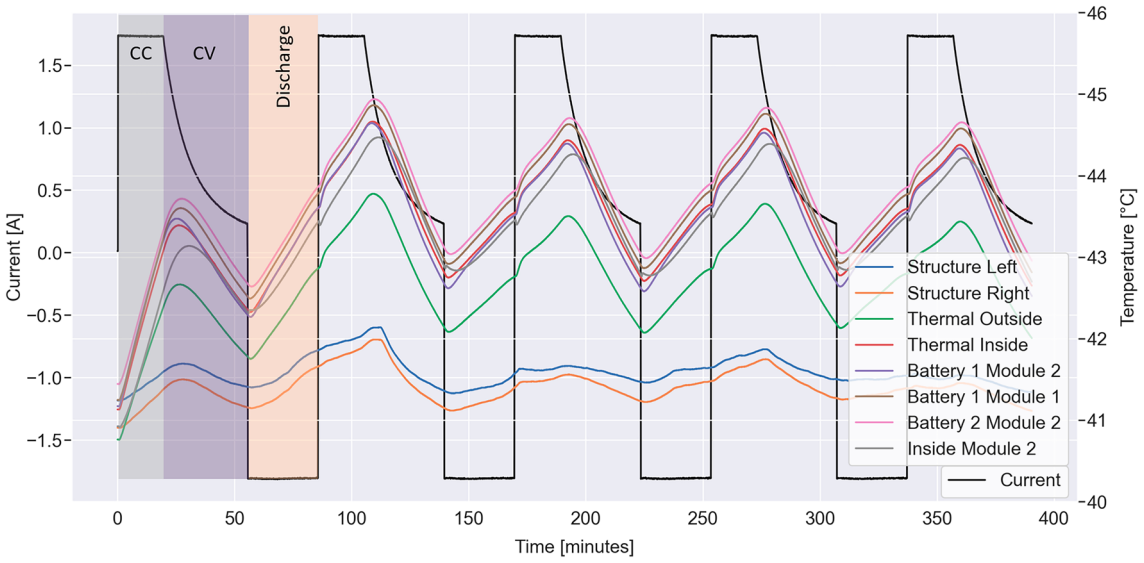

Fig. 8 Measured current (black) and temperatures (colours) over measuring time – Test with 40 °C baseplate, five cycles to show thermal equilibrium. Visible are the temperatures of the external sensors in order as shown in Fig. 6

During the test at 0 °C baseplate (with 3.5 A) the maximum difference is 5.5 K. The two sensors on the structure of the system experience a less pronounced increase in temperature over the test and also over the cycles themselves. The battery cells and the sensor on the top of the system have similar temperatures. Additionally, it can be seen that the battery cells differ in temperature by about 0.5 K. This might result from variations in their thermal connection to the system or from differences of the temperature sensors and their connection to the cells. Overall the temperature behaviour and the temperature difference of 5 K are acceptable. The thermal system is able to keep the temperatures in their specific ranges and removes the heat from the cells during operation.

In Table 4, the obtained cell temperature values for each conducted test are listed. For each test with a fixed baseplate temperature and current the minimum and maximum temperature are shown. In general, the temperatures are only below the operational limits at the beginning of the test due to the dwelling phase. Heating or discharging leads to an increase the temperature above 0 °C. The system can be operated between 0 °C and 40 °C up to 3.5 A. The testing with 10 A was not conducted at 40 °C as the limits were already hit at 20 °C. However, this test still can be seen as a successful a proof of concept for high power applications. The 10 A should only be used temporarily. Besides its influence on the temperature of the system the operation in high currents is expected to reduce the lifetime of the system.

4.2 Testing of functionality

Figure 9 shows the comparison of currents from the external source–sink and the onboard current sensor of one of the two modules. The current is shared between the two modules. The charging and discharging were carried out at 3.5 A. The measurement of the current sensor onboard is synchronous to the externally measured value consistently detecting half of the external current. The deviation lies below 1%,

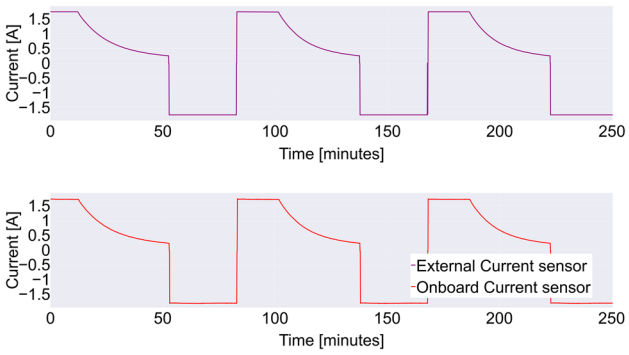

Fig. 9 External current sensor vs Onboard current sensor

which verifies the operation of the onboard current sensor in vacuum.

In a similar manner the measured voltages of the battery management and the source–sink were compared. Within the error ranges the values agree at all times.

Figure 10 shows the comparison of the onboard and external temperature sensor on cell 1. The stepped profile measured by the onboard temperature sensor arises from the lower resolution of the battery management's sensor. Nevertheless, the measured values of the two sensors do not deviate more than 0.4 K from each other. The offset could stem from the different types of sensors. A higher resolution for the onboard system is not needed for monitoring and the activation of heating. Additionally, it is observed that the software and communication is working appropriately.

4.3 Tests of functionality

The CAN communication worked flawlessly during the three weeks inside the vacuum chamber. No errors on the electronics or battery cells were observed over the three weeks of testing. The battery cell's voltages did not deviate from each other by more than 2%. Therefore, a need for cell

Table 4 Review of maximum and minimum temperatures of the onboard sensors for every test. Operations under the linits (blue) and over the limits (orange). At −20 °C and 55 °C the cells were only discharged

Baseplate Temperature [°C]	Current [A]	Maximum and Minimum Surface Temperature of the Cells [°C]															
		Cell 0		*Cell 1*		*Cell 2*		*Cell 3*		*Cell 4*		*Cell 5*		*Cell 6*		*Cell 7*	
		Max	*Min*	*Max*	*Min*	*Max*	*Min*	*Max*	*Min*	*Max*	*Min*	*Max*	*Min*	*Max*	*Min*	*Max*	*Min*
0	10A	33.1	-0.1	29.9	0	29.3	-0.1	34.7	-0.3	37.3	-0.2	33.3	-0.3	34.7	-0.3	40.1	-0.3
	3.5A	6.6	-0.4	5.4	-0.8	5.5	-0.7	7.2	-0.4	7.4	-0.3	6.2	-0.7	6.8	-0.5	8	-0.3
20	10A	49	20.6	46.1	18.8	45.5	18.9	50.3	21.1	52.3	21.2	48.9	19.6	49.8	20.2	54.4	21.3
	3.5A	25	21	24.3	20.8	24.3	20.8	25.4	21.1	25.6	21.2	24.8	20.8	25.1	21	25.9	21.3
40	3.5A	44.6	40.4	44.3	40.6	44.2	40.6	45	40.5	45.1	40.5	44.5	40.4	44.8	40.6	45.3	40.6
-20	3.5A DCH	-3.6	-21	-5.4	-22	-5.6	-22	-3.1	-21	-1.8	-21	-3.6	-22	-3.1	-21	-0.8	-20
55	3.5A DCH	60.7	54.8	60.3	55.9	60.3	55.8	61.1	54.6	61.3	54.8	60.8	55.6	60.9	55.6	61.4	54.5

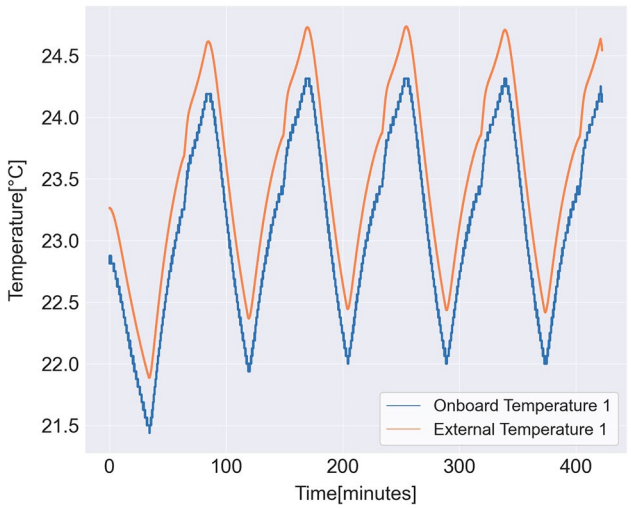

Fig. 10 External temperature sensor vs Onboard temperature sensor

balancing did not arise during the three weeks of charging and discharging.

During the test campaign the heaters were tested with a CAN command from outside and the operation of the system was monitored. The resulting temperature profile of the battery cells and the activity of the heater over time are shown in Fig. 11. The consumption of the heaters is at 0,7 W per module. The four heaters were able to increase the temperature of the system by around 0.75 K in 10 min. The temperature sensor recognizes the heater-on after one minute due to the distance between them. The heaters are working against the active cooling of the baseplate that is kept at 0 °C by a thermostat. If a cold start of the system below 0 °C occurs (during LEOP or emergency) discharging the system is fine as the operational limits are broader for discharging. After discharging the cells can only be charged if the operation was able to increase the cell temperature above 0 °C. Alternatively, the heater is able to lift up the initial cell temperature. During operation it can be assumed that the heating is able to keep cell temperatures above 0 °C if they start to drop below.

Cell balancing was also tested. The balancing of eight cells induces around 7 W of waste heat into the system. The balancing is generally only conducted at the end of a charge cycle on a few cells for several seconds. In this test the worst case was simulated and the balancing was continuously run for 30 min on all eight cells to see the heat development in case of a failure. The temperatures of the cells rise by around 12 °C to 15 °C in that timeframe.

5 Conclusions

A thermal vacuum test campaign was conducted on a COTS-based modular Li-ion battery system. The thermal behaviour of two battery modules with 28 V nominal voltage and eight battery cells each was investigated inside a vacuum chamber. The battery system was operated in temperatures from −20 °C to 55 °C in a high-vacuum for three weeks.

The thermal-vacuum (TVAC) test campaign proves the functionality of the battery system under LEO-relevant conditions. All cells worked properly during the tests. The dense system architecture with electronics between the cells the battery system was able to safely deliver power in a broad temperature range.

To verify the electronic functionality and working, external sensors were mounted to measure voltage, current and temperature values, the values from external sensors coincided with the values from sensor onboard. The software

Fig. 11 Operation of heater and influence on the battery cells

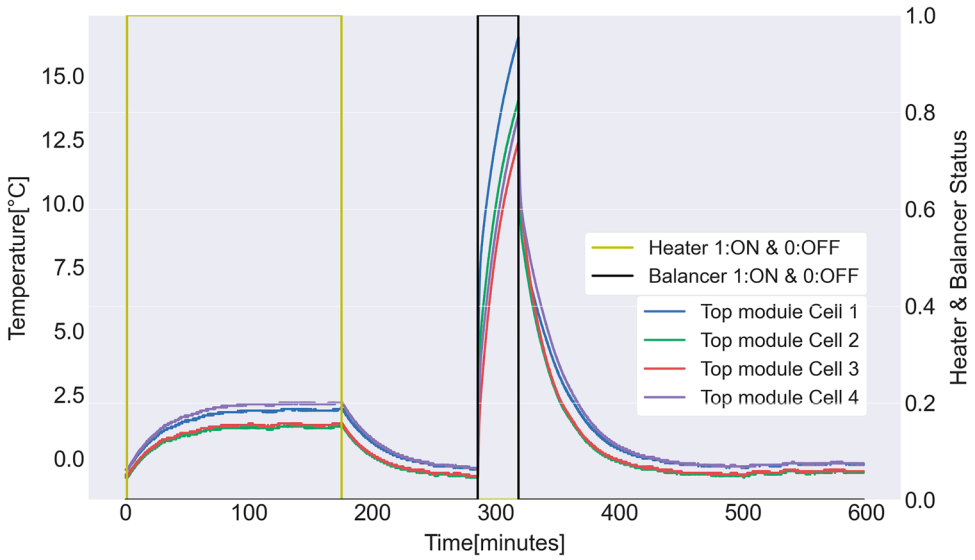

also worked properly and constantly delivered data and telemetry. It also processed external inputs. Throughout the test, the temperature of the battery cells was monitored.

The thermal management worked effectively and kept the battery cells in their temperature range. A temperature difference of around 5 K between the baseplate and the battery cells was observed during operation with 3.5 A. For higher currents the cell temperature increase is more pronounced resulting in a higher temperature difference between cell and base plate. The cell temperatures fell below the operating limits below 0 °C. Heating was tested for those temperatures. However, heating takes a long time to bring the cell temperatures up. Additionally, the heating tests were not sufficient to verify at which temperatures and for how long they would be able to raise the temperatures of the system.

For the tests with 3.5 A the limits were overshot at 40 °C baseplate temperature. The higher-power cycling with 10 A was only possible at 0 °C and 20 °C. The temperature behaviour seems to be in line with reports of other authors [30, 31].

Further investigation and research are essential to address safety and failure modes in the proposed battery system. Due to the inclusion of electronics and software it is crucial to ensure the system does not endanger the satellite's mission. Additionally, advancements on software and state estimation algorithms of the system need to be made. This will contribute to enhancing the overall performance and reliability of the battery system for satellite applications.

Moving forward, there are several aspects for future publications. The radiation test campaigns conducted on the electronic components of the system will be analyzed and published. Additionally, upcoming projects on low temperature missions and the integration of post-lithium battery cells (for specific applications) will leverage the scientific value of the presented modular battery system.

Acknowledgements Thanks to Martin Siemer from DLR-RY in Bremen for providing insight with a thermal analysis and thanks to Thilo Glaser from DLR-SY in Braunschweig for the support with the battery system's structure.

Funding Open Access funding enabled and organized by Projekt DEAL.

Data availability The data that support the findings of this study are available from the corresponding author, Marius Eilenberger, upon reasonable request.

Declarations

Conflict of interest The authors have no competing interests to declare that are relevant to the content of this article.

References

1. Knap, V., Vestergaard, L.K., Stroe, D.-I.: A review of battery technology in CubeSats and small satellite solutions. Energies **13**(16), 4 (2020). https://doi.org/10.3390/en13164097
2. Krause, F.C., Ruiz, J.P., Jones, S.C., Brandon, E.J., Darcy, E.C., Iannello, C., Bugga, R.V.: Performance of commercial Li-ion cells for future NASA missions and aerospace applications. J. Electrochem. Soc. (2021). https://doi.org/10.1149/1945-7111/abf05f
3. Pistoia, G.: Lithium-Ion Batteries: Advances and applications. 483–509
4. United Nations Conference on Trade and Development, Commodities at a Glance: Special issue on strategic battery raw materials. UN. (2020). https://doi.org/10.18356/9ba5e76c-en
5. Bisschop, R., Willstrand, O., Amon, F., Rosenggren, M.: Fire safety of lithium-ion batteries in road vehicles. RISE Report. RISE Research Institutes of Sweden. 50 (2019)
6. Pearson, C., Thwaite, C., Russel, N.: The use of small cell lithium-ion batteries for small satellite applications. (2004)
7. Kanevskii, L.S., Dubasova, V.S.: Degradation of lithium-ion batteries and how to fight it: a review. Russ. J. Electrochem. **41**, 1–16 (2005). https://doi.org/10.1007/s11175-005-0042-y
8. Genç, D., Thwaite, C.: Proba-1 and mars express: an ABSL lithium-ion legacy. (2011)
9. Barrea, T.P.: Spacecraft lithium-ion battery power systems. IEEE Press, Wiley, p.9 (2022). https://doi.org/10.1002/9781119772170.ch1
10. Ormston, T. et al.: Lithium ion battery management strategies for european space operations centre missions. SpaceOps 2014 Conference, Pasadena, CA: American Institute of Aeronautics and Astronautics, May 2014. https://doi.org/10.2514/6.2014-1883
11. Borthomieu, Y.: Satellite lithium-ion batteries. Elsevier, pp. 311–344. (2014). https://doi.org/10.1016/B978-0-444-59513-3.00014-5
12. GomSpace A/S, "NanoPower BP8 Datasheet", Rev.: 2.0.0, 21st of November 2022
13. Funase, R., Nakamura, R., Nagai, Y., Enokuchi, M.: Development of COTS-based pico-satellite bus and its application to quick and low cost on-orbit demonstration of novel space technology. Trans. JSASS Space Tech. Japan **6**, 1–9 (2008). https://doi.org/10.2322/tstj.6.1
14. ECSS Secretatriat, "Li-ion battery testing handbook", ECSS-E-HB-20–02A, 1st of October 2015
15. Aung, H.H., Low, K., Goh, S.T.: Modeling and state of charge estimation of a lithium ion battery using unscented Kalman filter in a nanosatellite. 9th IEEE Conference on Industrial Electronics and Applications. 1422–1426 (2014). https://doi.org/10.1109/ICIEA.2014.6931391
16. Bolay, L.J., Schmitt, T.W., Mendoza-Hernandez, O.S., Sone, Y., Latz, A., Horstmann, B.: Degradation of lithium-ion batteries in aerospace. European Space Power Conference. p. 1–3 (2019). https://doi.org/10.1109/ESPC47532.2019.9049261.

17. SatSearch Website, Satellite->Power->Battery, Accessed: 14/08/2022, Available: https://satsearch.co/products/categories/satellite/power/battery
18. NANOeps with 158Wh battery pack (nano-eps-158w-1), sky-labs. (2022). Available: https://www.skylabs.si/products/electrical-power-system/
19. NanoPower BPX, Gomspace. (2022). Available: https://gomspace.com/shop/ subsystems/ power/nanopower-bpx.aspx
20. CubeSat Kit™ Battery Module 2 (BM 2), Pumpkin Space Systems. (2022) Available: https://www.pumpkinspace.com/store/p198/Intelligent_Protected_Lithium_Battery_Module_with_SoC_Reporting_%28BM_2%29.html
21. Pearson, C., Thwaite, C., Curzon, D., Rao, G.: The long-term performance of small-cell batteries without cell-balancing electronics. NASA Battery Power Workshop (2004)
22. Eilenberger, M., Gunasekar, H., Gomez Toro, D., Gentner, C. Development and qualification of a scalable and modular COTS-based Li-ion battery system for satellites in low earth orbit, IAC Paris (2022)
23. Howell et al. Thermal radiation heat transfer. (2016)
24. Escobar, E., Diaz, M., Zagal, J.C.: Design automation for satellite passive thermal control. In The 4S Symposium, pages 1–10 (2012)
25. Hengeveld, D., Mathison, M.; Groll, E., Braun, J., Williams, A.: Review of modern spacecraft thermal control technologies, 180–210 (2010). https://doi.org/10.1080/10789669.2010.10390900
26. ECSS Secretariat, "Space engineering testing", ECSS-E-ST-10–30C, 31st of May 2022
27. ECSS Secretariat, "Space engineering Thermal control general requirements", ECSS-E-ST-31C, 15th of November 2008
28. Ji, Y., Zhang, Y., Wang, C.-Y.: Li-ion cell operation at low temperatures. J. Electrochem. Soc. **160**(4), A636–A649 (2013). https://doi.org/10.1149/2.047304jes
29. Ma, S., Jiang, M., Tao, P., Song, C., Wu, J., Wang, J., Deng, T., Shang, W.: Temperature effect and thermal impact in lithium-ion batteries: a review. Prog. Natl. Sci. Mater. Int. **28**(6), 653–666 (2018). https://doi.org/10.1016/j.pnsc.2018.11.002
30. Jacques, L.: Thermal Design of the Oufti-1 nanosatellite. (2009)
31. Doyle, M., Gloster, A., Griffin, M., Hibbett, M.J., Kyle, J., O'Toole, C., Mangan, J., Murphy, D., Wong, N.L., Akarapu, S.K., Dunwoody, R., Erkal, J., Finneran, G., Reilly, J., Salmon, L., Thompson, J.W., Walsh, S., Shortt, B., Martin-Carrillo, A., McBreen, S., McKeown, D.J., O'Connor, W.J., Uliyanov, A., Wall, R., Hanlon, L.: Design, development and testing of flight software for EIRSAT-1: a university-class CubeSat enabling astronomical research. J. Astron. Telescopes Instrum. Syst. **9**, 017002–017002 (2023). https://doi.org/10.3390/aerospace9020099